IDA PAPER P-3084

ERROR ANALYSIS FOR BULLET TRACKER CONCEPT

Jeffrey Nicoll
David Sparrow

19960730 066

August 1995

Prepared for
Office of the Secretary of Defense for Program Analysis and Evaluation
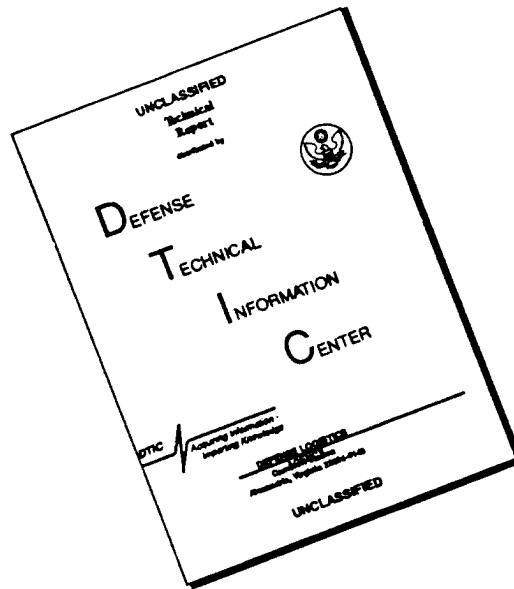(Land Forces Division)

IDA

INSTITUTE FOR DEFENSE ANALYSES
1801 N. Beauregard Street, Alexandria, Virginia 22311-1772

DISCLAIMER NOTICE

THIS DOCUMENT IS BEST QUALITY AVAILABLE. THE COPY FURNISHED TO DTIC CONTAINED A SIGNIFICANT NUMBER OF PAGES WHICH DO NOT REPRODUCE LEGIBLY.

IDA PAPER P-3084

ERROR ANALYSIS FOR BULLET TRACKER CONCEPT

Jeffrey Nicoll
David Sparrow

August 1995

IDA

INSTITUTE FOR DEFENSE ANALYSES

CONTENTS

TABLES

FIGURES

v

SUMMARY

It has been proposed that a single staring infrared focal plane array sensor be used to measure the track of a sniper bullet and used to deduce the location of the shooter. This involves deducing the three-dimensional track from the two-dimensional information provided on the focal plane. This would be impossible in the absence of gravity or other forces since an infinite number of straight line, constant velocity three-dimensional trajectories correspond to the same two-dimensional track: a slowly moving object at short range leaves the same track as a more distant object moving more rapidly in a parallel direction. However, in the presence of gravity, the trajectory is curved and this curvature can be used, in principle, to distinguish the tracks. The proposed system has been partly demonstrated in simulation but no complete error analysis was done. This paper provides that error analysis and therefore gives bounds on the sensor performance required to reach any specified degree of performance.

Exact maximum likelihood estimates of the errors are provided for four cases:

(i) Zero drag crossing shots. A crossing shot is defined as one which passes through the sensor field of view perpendicular to the axis of the sensor. This is the simplest example to understand and the exact error can be calculated.

(ii) Zero drag non-crossing shot. The projectile either approaches the sensor or recedes from it. A lower bound for the error is given (that is, the true error is larger than that calculated) that is expected to be accurate under reasonable conditions.

(iii) Crossing shot with drag. Now a linear drag force is added. The primary effect of the drag is to slow the projectile and therefore leave it in the field of view longer. Again an accurate lower bound for the error is calculated.

(iv) Non-crossing shot with drag. In the first three cases, explicit elementary functions are calculated for the maximum likelihood estimate of the range error; in this most general case, a lower bound of the error is given.

A sample result is given for the crossing shot with linear drag. The error in down-range location, δy_0, for a shot crossing a field of view, Ω, is given by:

$$(\delta y_0)^2 = \{ 720\, \sigma^2\, \bar{u}_0{}^5 / [g^2 R\, y_0\, (2 \tan (\Omega/2))^5] \} f$$

where

σ = single pixel measurement error (radians)

R = update rate of the sensor (Hz)

g = 9.8 m/sec^2

y_0 = down-range distance

$\bar{u}_o$ = average velocity of projectile

f = 1 + weak function of the drag.

A similar estimate is derived for other than crossing shots. It is also shown that the other trajectory parameters can be estimated extremely accurately so that the error in location induced by the other errors may be neglected. For the most favorable condition, a shot crossing the entire field of view, a sensor with the following nominal characteristics:

σ = 0.5 milliradians

Ω = 60 degrees

R = 400 Hz

y_0 = 250 meters

$\bar{u}_o$ = 600 meters/sec

one has $\delta y_0 = \pm 27$ meters with proportionally larger or smaller errors with different choices of parameters. If, in addition, the muzzle flash is unobserved, there may be an error in extrapolating the track origin back to a presumed location. Even a 0.1 second uncertainty in the time of the shot gives a 100 meter error corresponding to an error box of 50×100 meters.

The error depends on the -5/2 power of the time in the field of view. For example, if the trajectory is only observable over 30 degrees rather than 60, the error increases to ± 150 meters. In urban or other cluttered environments the field of view may be sharply restricted. If the observable portion of the trajectory is restricted to 60 meters with an average velocity of 600 meters/sec, the range error at a range of 100 meters is ± 220 meters and increases quadratically with range.

The range error estimate given is a lower bound to the error since a variety of perturbations were neglected that, in principle, increase the error. These include atmospheric perturbations, tumbling of the bullet, bullet lift and crosswind sensitivity. Nor are any detailed infrared sensor considerations other than resolution included.

I. INTRODUCTION

Knowledge of the location of a sniper, even incomplete knowledge, may be militarily useful in a variety of scenarios of concern to the Department of Defense in both combat operations and operations other than war. There are a number of complex issues to be sorted out which depend upon terrain, rules of engagement, and tolerance for collateral damage before any particular implementation of sniper location and sniper neutralization technology can be reasonably fielded. We acknowledge these issues and their importance. However, resolution of these global issues depends in part on an accurate assessment of the technical capabilities of the particular implementations. In this paper, we present a calculation of the uncertainty in determining the three-dimensional location of a sniper, constructed from a two-dimensional track of the bullet.

Specifically, it has been proposed that a staring infrared focal plane array sensor be used to measure the track of a sniper bullet and used to deduce the location of the shooter. This involves deducing the three-dimensional track from the two-dimensional information provided on the focal plane. This would be impossible in the absence of gravity or other forces since an infinite number of straight line, constant velocity three-dimensional trajectories correspond to the same two-dimensional track: a slowly moving object at short range leaves the same track as a more distant object moving more rapidly in a parallel direction. However, in the presence of gravity, the trajectory is curved and this curvature can be used, in principle, to distinguish the tracks.

There have been simulation results that indicate that a relatively simple infrared sensor might be able to perform this task. In particular a staring focal plane array sensor of 512×512 pixels covering a field of view of 60 degrees (approximately 1 radian) with a readout rate of 400 Hz has been proposed as sufficient for the task. The pixel size of this sensor would be 2 milliradians (mr) which is relatively coarse. However, it is also suggested that the blurred and streaked image of the projectile could be analyzed to provide subpixel accuracy in the centroid location of the object. Although a detailed analysis has not been presented, a figure of "1/4 pixel" or 0.5 milliradians has been put forward as an

estimate of the single pixel measurement accuracy.[1] Note that this is not the overall track accuracy, which is improved as the number of data points measured increases, but is the individual measurement error. If the single pixel measurement error is 1/2 pixel or 1 milliradian, the range errors will double.

In order to provide a basic understanding of the error mechanisms for this problem, a maximum likelihood estimate is made for four cases of increasing complexity:

(i)   Zero drag crossing shots. A crossing shot is defined as one which passes through the sensor field of view perpendicular to the axis of the sensor field of view. This is the simplest example to understand and the exact error can be calculated.

(ii) Zero drag non-crossing shot. The projectile either approaches the sensor or recedes from it. A lower bound for the error is given (that is, the true error is larger than that calculated) that is expected to be accurate under reasonable conditions.

(iii) Crossing shot with drag. Now a linear drag force is added. The primary effect of the drag is to slow the projectile and therefore leave it in the field of view longer. Again a lower bound for the error is calculated.

(iv) Non-crossing shot with drag. In the first three cases, explicit elementary functions are calculated for the maximum likelihood estimate of the range error; in this most general case, an exact solution for a lower bound of the error is given in terms of a quadrature.

It will be assumed for convenience that the focal plane array is aligned perfectly with the local direction of gravity. It will be generally assumed that the trajectory is nearly horizontal so that the horizontal (azimuthal) component of the velocity is much greater than the vertical (elevation) component. This is consistent with the imagined scenario of a sniper; even if located in a building 20 meters above ground level, firing at a range of 400 meters gives a ratio of vertical to horizontal components of 1/20.

Zero drag is considered in Section II. This case defines all of the basic ideas and is easy to follow. The simplest case is the crossing shot which is parallel to the plane of the sensor. In this case, the azimuthal and elevation degrees of freedom decouple. Only the elevation degrees of freedom are relevant to the determination of the range to the target. Maximum likelihood, in this case, is equivalent to a least squares approach. Section IIB

---

[1] In the absence of a complete sensor design, the single pixel measurement accuracy and sample rate will be taken as quoted; the results can easily be scaled to different values. Appendix B gives a brief discussion of sensor issues.

describes the estimate of the range error in this case. The maximum likelihood estimate of the error is considerably larger than a naive estimate of the error due to the strong correlation of two of the parameters to be estimated: the gravitation drop and the vertical component of the velocity. The basic idea is that it is hard to separate the small vertical displacement on the focal plane due to gravity from the displacement due to a slightly depressed trajectory. Section IIC gives the errors for the remaining trajectory parameters and shows them to be small. Section IID generalizes the previous results to the non-crossing case. The error is reduced for approaching shots and increased for receding shots; this can be understood as a magnification or demagnification effect. In the most extreme limit of an approaching shot that passes very near the sensor, the range error is reduced to about 30 percent of the crossing shot case.

In Section III, the effects of drag are introduced. A linear drag model is used for mathematical convenience and because it is an excellent representation of the forces on the projectile in the relevant domain. Within this model, the primary effect of the drag is to slow down the projectile, therefore increasing the amount of time it stays within the field of view of the sensor, which in turn has two consequences: (1) greater statistical accuracy from the larger number of data points; (2) a longer time for gravity to act on the projectile. In general, the drag coefficient must be estimated from the data; this couples the horizontal and vertical track parameters. However, for nearly horizontal trajectories, it can be shown (Section III-B) that the horizontal data provides a sufficiently accurate estimate of the drag force that errors in the drag coefficient are not the limiting error mechanism. The maximum likelihood estimate of the range can again be made using only the vertical measurements, assuming that drag force is known exactly. In Section III-C, a similar result to the no-drag case is obtained for the crossing shot with the average velocity in the field of view replacing the initial (and essentially) constant velocity in the no-drag case. Section III-D combines the drag model with the approaching shot.

This paper will focus on the estimate of the three-dimensional track parameters from the two-dimensional sensor data. This attempts to provide a location in three-dimensional space of the first point of the measured track. This is not the only source of error in locating the shooter if the initial portion of the track (including the muzzle flash) is not part of the measured track. If the flash is not observed, there is a further error in extrapolating the track backwards by an unknown time. This extrapolation error may be large and is proportional to the product of the time between the flash and the first observation Δt and the

muzzle velocity, u_0, which is itself uncertain.[2] In some scenarios, this is the dominant error in the problem and may be more important operationally than the statistical error discussed in the following sections; note that a 0.1 second error in the time may correspond to as much as a 100 meter error in the location. For crossing shots the extrapolation error is orthogonal to the range estimate. In an urban environment and a crossing shot, the range from the sensor is important in determining from which street a shot is fired; the extrapolation error indicates how far down that street the shooter is. It may be sufficient to identify the street. On the other hand, for a shot directed toward the sensor the ranging error and the extrapolation error are in the same direction and the error in identifying the street is larger.

---

2 The muzzle velocity varies with the type of weapon and ammunition over a broad range. The velocity is estimated in the course of the overall estimation but is subject to the same uncertainties as the range.

II. ZERO DRAG

A. ZERO DRAG MOTION

The position of a projectile influenced only by gravity is given in Cartesian coordinates by:

$$x_i = x_0 + u_{x0}t_i \qquad \text{(II-1a)}$$

$$y_i = y_0 + u_{y0}t_i \qquad \text{(II-1b)}$$

$$z_i = z_0 + u_{z0}t_i - \frac{g}{2}t_i^2 \quad , \qquad \text{(II-1c)}$$

where the axes are chosen so that the y direction is the direction perpendicular to the sensor. The N values of the time coordinate, t_i, are evenly spaced from 0 to t, where $t_1 = 0$ and $t_N = t$, the total time in the field of view of the sensor. The measured pixel coordinates are given by the ratio of these quantities:

$$X_i = \frac{x_0 + u_{x0}t_i}{y_0 + u_{y0}t_i} + \eta_{xi} \qquad \text{(II-2a)}$$

$$Z_i = \frac{z_0 + u_{z0}t_i - \frac{1}{2}gt_i^2}{y_0 + u_{y0}t_i} + \eta_{zi} \quad , \qquad \text{(II-2b)}$$

where η_{xi} and η_{zi} are the errors in the pixel measurements. Assuming that the errors are independent and normally distributed,[3] with σ_x and σ_z the standard deviations, the estimation of the unknown parameters may be performed by maximum likelihood or equivalently, least squares. The total square error around the assumed track is

$$E = \sum_{i=1,N} [Z_i - \frac{z_0 + u_{z0}t_i - \frac{1}{2}gt_i^2}{y_0 + u_{y0}t_i}]^2 / 2\sigma_z^2 + [X_i - \frac{x_0 + u_{x0}t_i}{y_0 + u_{y0}t_i}]^2 / 2\sigma_x^2 \quad . \qquad \text{(II-3)}$$

---

[3] Some care must be taken with this assumption. Appendix B shows that for a severely undersampled sensor for which a single point error of 0.3 is appropriate, the errors are not independent and the full value of N does not apply.

Note that if $\sigma_x = \sigma_z$, then the error is isotropic and independent of the coordinate system.[4]

B. RANGE ERROR FOR CROSSING SHOTS

The maximum-likelihood estimate couples all the unknown parameters x_0, y_0, z_0 and u_{x0}, u_{y0}, and u_{z0}, giving a 6-parameter nonlinear estimation. Note that only the presence of the gravitational term permits a solution since otherwise the problem is homogeneous in the positions and velocities and no unique solution can be found. Thus, it is the size of the gravitational term and its separability from the other terms, in particular, the z-component of the velocity, that sets the scale of the error.

Although it is possible to address the full non-linear estimation problem directly, it is more illuminating to consider the special case of the crossing shot with $u_{y0} = 0$. In this case, the remaining 5-parameter estimation problem in $x' = x_0/y_0$, $z' = z_0/y_0$, $v_{x0} = u_{x0}/y_0$ $v_{z0} = u_{z0}/y_0$ and $g' = g/2y_0$ is linear. Moreover, the azimuthal variables x' and v_{x0} are decoupled from the elevation variables z', v_{z0} and g', separating the 5-parameter estimate problem into a 2-parameter estimate for the azimuthal variables and a 3-parameter estimate for the elevation variables. All of the absolute range information is in the variable g' since the other four parameters are homogeneous in range, representing angular positions on the focal plane or angular velocities.

The problem is simplified by the fact that the time coordinates are uniformly spaced. For a high speed sensor (sampling rate, $R = 100$ Hz or greater), the sums of various powers of t_i can be represented by integrals.

$$< t_i^m > = 1/N \, \Sigma \, t_i^m = t^m/(m+1) \quad . \tag{II-5}$$

The values of the parameters to be estimatedfor the 3-parameter elevation variables are determined by solving the linear equations given by the first derivatives of the error.

$$0 = -N(< Z_i > - z' - v_{x0} <T_1 > + g'< T_2 >)/ \sigma^2 \tag{II-6a}$$

$$0 = -N(<T_1 Z_i > - z' < T_1 > - v_{x0} < T_1{}^2 > + g'< T_1 \, T_2 >)/ \sigma^2 \tag{II-6b}$$

$$0 = N(< T_2 Z_i > - z' < T_2 > - v_{x0} < T_1 \, T_2 > + g'< T_2{}^2 >)/ \sigma^2 \quad , \tag{II-6c}$$

---

[4] It is not assumed in this paper that the error is the same in the vertical and horizontal directions. In fact, since for a nearly horizontal shot moving at 1 radian/sec or more over the focal plane (thereby staying in the same vertical row of pixels between samples but being smeared over 2 or more pixel subtenses horizontally), it is unlikely that they are the same. Only the value of the vertical error is of importance in this paper as long as the error in the horizontal estimate is on the order of 1–2 milliradians or less.

where, for notational convenience, σ has been written for σ_z, the single pixel measurement error in the vertical direction. For future use, the notation, $T_1 = t$ and $T_2 = t^2$ is introduced.

Of more interest is the matrix of second derivatives that determines the error.

$$M = N/\sigma^2 \begin{vmatrix} 1 & <T_1> & -<T_2> \\ <T_1> & <T_1^2> & -<T_1 T_2> \\ -<T_2> & -<T_1 T_2> & <T_2^2> \end{vmatrix} \qquad \text{(II-7a)}$$

or numerically:

$$M = N/\sigma^2 \begin{vmatrix} 1 & t/2 & -t^2/3 \\ t/2 & t^2/3 & -t^3/4 \\ -t^2/3 & -t^3/4 & t^4/5 \end{vmatrix} \qquad \text{(II-7b)}$$

Since the estimation problem is linear, the covariance matrix is independent of the values of the parameters to be estimated. Note that the second and third lines of the matrix are nearly proportional, indicating that the estimates for the z-velocity and the gravitational term are highly correlated; this correlation is important for computing the total variance in the estimate of g', $(\delta g')^2$.

The total variance of the estimates of the parameters is given by the diagonal elements of the inverse of the covariance matrix. The variance in the vital estimate of g' is

$$(\delta g')^2 = \frac{\sigma^2}{N\sigma_2^2(1-\rho^2)} \qquad \text{(II-8)}$$

where

$$\sigma_1^2 = <T_1^2> - <T_1>^2 \qquad \text{(II-9a)}$$

$$\sigma_2^2 = <T_2^2> - <T_2>^2 \qquad \text{(II-9b)}$$

$$\rho^2 = [<T_1 T_2> - <T_1><T_2>]^2/\sigma_1^2 \sigma_2^2 \quad , \qquad \text{(II-9c)}$$

or numerically:

$$\sigma_1^2 = (1/12) t^2 \qquad \text{(II-10a)}$$

$$\sigma_2^2 = (4/45) t^4 \qquad \text{(II-10b)}$$

$$\rho^2 = 15/16 \quad , \qquad \text{(II-10c)}$$

giving finally for the variance in the estimate of g':

$$(\delta g')^2 = 180 \, \sigma^2 / (N \, t^4) \quad . \tag{II-11}$$

The form of this equation is as expected from general considerations and dimensional analysis, but the numerical factor of 180 is larger than might be intuitively expected, corresponding to the strong correlation[5] between the gravitational and the z-component of the velocity terms.

The variance in g' can be translated into the variance in the estimate in the range, y_0:

$$(\delta y_0)^2 = 180 \, \sigma^2 \, y_0^4 / (N(g/2)^2 \, t^4) \quad . \tag{II-12}$$

One way of understanding this error is to consider the fractional error, written in terms of the angular change induced by the gravitational drop $\delta\Theta = gt^2/2y_0$:

$$(\delta y_0/y_0)^2 = 180 \, \sigma^2 / (N \, \delta\Theta^2) \quad . \tag{II-13}$$

Since for a 400 Hz sensor, the value of N is on the order of 400 or less, a small fractional error in range will in general require that the single pixel measurement error, σ, must be much less than the gravitational drop, $\delta\Theta$, to get an accurate range estimate. For example, for N = 400, a 10-meter accuracy at 1 km would require $\sigma \approx \delta\Theta / 70$. For a 1 second flight at 1 km, $\delta\Theta \approx 5$ milliradian, requiring a single pixel accuracy of less than 0.07 milliradian.

Returning to Eq. (II-12), it can be written as

$$(\delta y_0)^2 = 180 \, \sigma^2 \, y_0^4 / (R(g/2)^2 \, t^5) \quad , \tag{II-14}$$

where R is the sample rate. The total time for a projectile that crosses the entire field of view is related to the range y_0 and field of view Ω of the sensor.

$$y_0 \, 2 \tan (\Omega/2) = u_{x0} \, t \sim u_0 \, t \quad , \tag{II-15}$$

where u_0 is the projectile velocity in meters/sec. Therefore

$$(\delta y_0)^2 = 720 \, \sigma^2 u_0^5 / [g^2 \, R \, y_0 \, (2 \tan (\Omega/2))^5] \quad . \tag{II-16}$$

---

[5] It might be naively assumed that the confusion between the z-component of the velocity and the drop induced by gravity can be transformed away by choosing a coordinate system aligned along the projectile's initial velocity. In this case the gravity terms appear isolated as the only forces transverse to the direction of motion. If one could do this, the factor of 180 would be reduced by a factor of 16, improving the range estimates by a factor of 4 (if the origin of the track is likewise transformed away, the total reduction in the variance is from 180 to 5). This, however, is an illusion. Although one may imagine transforming to such a coordinate frame, in fact one has to estimate the parameters of that transformation since the depression angle of the gun is unknown. This estimate is mathematically identical to the estimation procedure used here and gives rise to the same correlated errors.

The range variance is inversely proportional to the range and proportional to the fifth power of the projectile velocity. For shots which originate within the field of view, the time is reduced and the error increases rapidly. For example if the trajectory occupies only 1/2 of the field of view, the variance increases by a factor of $2^5 = 32$. In many environments (for example, urban warfare) a reduction in the field of view many be expected.

Using the assumed sensor parameters

$$\sigma = 0.5 \text{ milliradians} \tag{II-17a}$$

$$\Omega = 60 \text{ degrees} \tag{II-17b}$$

$$R = 400 \text{ Hz} \tag{II-17c}$$

one has

$$\delta y_0 \approx \pm 48 \text{ m } [(60/\omega)^5 u_0^5 / y_0]^{1/2} \ , \tag{II-18}$$

where ω is the amount of the trajectory that is visible in degrees ($\omega \leq 60$), u_0 is measured in km/sec, and y_0 in km. (For convenience, the values of u_0 and y_0 are given in meters in the tables that follow.) The error is large for high velocity projectiles with u_0 of order 1 km/sec. Of course, the numerical value of the coefficient depends on the sensor parameters chosen. Table II-1 gives the range error for a number of parameter choices (Appendix A gives the muzzle velocity of a number of rifles; they range from 700 to over 1,000 meters/sec). For low velocity bullets the range errors are reduced but are still significant especially if only 30 degrees of the field of view is available.

Table II-1. Range Errors for Different Parameters

Projectile velocity (m/sec) and range (m)	60 degree available	30 degree available
$u_0 = 600$ $y_0 = 250$	$\delta y_0 \approx \pm 27$ m	$\delta y_0 \approx \pm 150$ m
$u_0 = 600$ $y_0 = 1,000$	$\delta y_0 \approx \pm 13.5$ m	$\delta y_0 \approx \pm 75$ m
$u_0 = 800$ $y_0 = 250$	$\delta y_0 \approx \pm 55$m	$\delta y_0 \approx \pm 310$ m
$u_0 = 800$ $y_0 = 1,000$	$\delta y_0 \approx \pm 27.5$m	$\delta y_0 \approx \pm 155$m
$u_0 = 1,000$ $y_0 = 250$	$\delta y_0 \approx \pm 96$ m	$\delta y_0 \approx \pm 540$ m
$u_0 = 1,000$ $y_0 = 1,000$	$\delta y_0 \approx \pm 48$ m	$\delta y_0 \approx \pm 270$ m

C. ESTIMATES OF THE OTHER TRAJECTORY PARAMETERS

The same maximum likelihood estimates used for the range error provide estimates for the other trajectory parameters. This section summarizes those results and shows that the projective track parameters are estimated to acceptable accuracies under almost all conditions.

The error in the vertical angular velocity, δv_z is

$$(\delta v_z)^2 = \frac{\sigma_z^2}{N\sigma_1^2(1-\rho^2)} \quad \text{or} \quad (\delta v_z)^2 = \frac{192\sigma_z^2}{Nt^2} \quad . \tag{II-19a}$$

The large numerical factor is again a consequence of the large correlation between this parameter and the gravitational term. For a crossing shot covering the entire field of view, $v_x t = 2 \tan(\Omega/2)$, so this can be rewritten as:

$$\frac{(\delta v_z)^2}{v_x^2} = \frac{192\sigma_z^2}{N(2\tan(\Omega/2))^2} \quad . \tag{II-19b}$$

Since it may be assumed that $N \geq 35$, the error in the depression angle of the track is

$$\frac{\delta v_z}{v_x} \leq 2\sigma_z \approx 10^{-3} \quad . \tag{II-19c}$$

Even with a path length of 1 km, this 1 milliradian error in the depression angle of the trajectory is equivalent to an error of less than 1 meter.

The error in the initial elevation coordinate $\delta z'$ is

$$(\delta z')^2 = \frac{\sigma_z^2[<T_1^2><T_2^2>-<T_1T_2>]}{N\sigma_1^2\sigma_2^2(1-\rho^2)} \quad \text{or} \quad (\delta z')^2 = \frac{9\sigma_z^2}{N} \quad . \tag{II-20a}$$

If it is assumed that $N \geq 35$, the error in the initial elevation of the track is

$$\delta z' \leq \sigma_z/2 \approx 0.25 \ 10^{-3} \quad . \tag{II-20b}$$

For a path length of 1 km, this 1/4 milliradian error is equivalent to an error of less than 0.25 meter.

For the azimuthal coordinates, the results are of a similar form with smaller numerical coefficients (since only two parameters are estimated).

$$(\delta v_x)^2 = \frac{\sigma_x^2}{N\sigma_1^2} \quad \text{or} \quad (\delta v_x)^2 = \frac{12\sigma_x^2}{Nt^2} \quad . \tag{II-21a}$$

For a crossing shot crossing the entire field of view, $v_x t = 2 \tan(\Omega/2)$:

$$\frac{(\delta v_x)^2}{v_x^2} = \frac{12\sigma_x^2}{N(2\tan(\Omega/2))^2} \quad . \qquad \text{(II-21b)}$$

Again assuming that $N \geq 35$, the relative error in the azimuthal velocity of the track is

$$\frac{\delta v_x}{v_x} \leq \frac{\sigma_x}{2} \approx 0.25 \; 10^{-3} \quad . \qquad \text{(II-22)}$$

The azimuthal velocity is on the order of 1 radian/sec; therefore, the error is less than 0.25 mr/sec.

The error in the initial azimuthal coordinate $\delta x'$ is

$$(\delta x')^2 = \frac{\sigma_x^2 <T_1^2>}{N\sigma_1^2} \quad \text{or} \quad (\delta x')^2 = \frac{4\sigma_x^2}{N} \quad . \qquad \text{(II-23a)}$$

If it is assumed that $N \geq 35$, the error in the initial elevation of the track is

$$\delta x' \leq \sigma_x / 3 \approx 0.17 \; 10^{-3} \quad . \qquad \text{(II-23b)}$$

For ranges of the order of 1 km, this gives an error of less than 1/6 meter.

Thus, for shots covering the entire field of field, the errors in the projective coordinates of the track origin and the trajectory angles are known to 1 part in 1,000 or better. For trajectories that occupy only a fraction of the field of view, the errors increase but are still likely to be acceptably small. The error in range is larger in distance units since the physical scale of the drop due to gravity is so small, compared either to the entire field of view or to the single pixel measurement error.

D. NON-CROSSING SHOTS

1. Estimate of the Closing Velocity

The high quality of the estimates for the projective track parameters allows a simple extension to the non-crossing case. In general, one would have to solve the coupled azimuthal and elevation equations (a 6×6) problem, but as will be shown in this section, the azimuthal equations alone give a sufficiently precise estimate of the projective velocity in the y-direction (toward or away from the sensor), $v_{y0} = u_{y0}/y_0$. Then, the error in the elevation equations can be analyzed assuming that the value of v_{y0} is exactly known. The true error will be somewhat larger than this but not significantly so.

One could solve the azimuthal estimation problem exactly; however, since only the precision of the estimate is in question, a simpler perturbational approach suffices. Begin with the azimuthal pixel value equation from (II-2a) above.

$$X_i = \frac{x_0 + u_{x0}t_i}{y_0 + u_{y0}t_i} + \eta_{xi} \quad . \tag{II-24a}$$

Using the projective coordinates, this may be expanded in a power series if v_y t is small (a close to crossing shot):

$$X_i = \frac{x' + v_x t_i}{1 + v_y t_i} + \eta_{xi} = x' + (v_x - x' v_y)t_i - v_y v_x t_i^2 + O(v_y^2 t_i^2) + \eta_{xi} \quad . \tag{II-24b}$$

This is formally identical to the 3-parameter estimation problem for the elevation variable in the crossing-shot case with relabeled coefficients. Therefore, one has immediately that:

$$(\delta v_x v_y)^2 = \frac{\sigma^2}{N\sigma_2^2(1 - \rho^2)} = \frac{180\sigma^2}{Nt^4} \quad . \tag{II-24c}$$

For a crossing shot covering the entire field of view, $v_x t = 2 \tan (\Omega/2)$, so using the fact that v_x is well estimated, this can be rewritten as

$$\frac{(\delta v_y)^2}{v_x^2} = \frac{180\sigma^2}{N[2\tan(\Omega/2)]^4} \quad . \tag{II-24d}$$

For $N \geq 35$, this gives an error in the bearing of the trajectory $\delta v_y/v_x$ of:

$$\delta v_y/v_x < 1.7 \, \sigma \approx 10^{-3} \quad . \tag{II-24e}$$

Even if the field of view is reduced to 30 degrees, the error only increases to 4×10^{-3}. Thus, the projective y-coordinate of the velocity can be assumed to be well known. Although this estimate was formed perturbatively, it is clear that the error in the projective y velocity will remain small in most scenarios. It will therefore be assumed to be known for the purpose of analyzing the elevation error.

2. Estimates of Range

Examining the error and assuming v_y is a known quantity, one sees that the estimation problem is still linear, but the averages are now weighted with the factor of $1/(1+v_y t)^2$. Define the average of any function of time, $<h(t)>$, by

$$< h(t) > = \frac{1 + v_y t}{t} \int_0^t \frac{dt}{(1 + v_y t)^2} h(t) \quad , \tag{II-25a}$$

II-8

then the range error is given by

$$(\delta g')^2 = \frac{(1+v_y t)\,\sigma_z^2}{N\sigma_2^2(1-\rho^2)} \quad \text{or} \quad (\delta y_0)^2 = \frac{(1+v_y t)\,y_0^4\,\sigma_z^2}{N\,(g/2)^2\sigma_2^2\,(1-\rho^2)} \quad , \qquad \text{(II-25b)}$$

where the standard deviations and correlation coefficients are computed using the average of Eq. (II-25a). The averages of the various powers of t are given by:

$$< t >=< T_1 >= t\,[1-\frac{1+z}{z^2}(z-\ln(1+z))] \qquad\qquad \text{(II-26a)}$$

$$< t^2 >=< T_2 >=< T_1^2 >= t^2\,[1-2\frac{1+z}{z^3}(-z+\frac{z^2}{2}+\ln(1+z))] \qquad \text{(II-26b)}$$

$$< t^3 >=< T_1 T_2 >= t^3\,[1-3\frac{1+z}{z^4}(z-\frac{z^2}{2}-\ln(1+z))] \qquad\qquad \text{(II-26c)}$$

$$< t^4 >=< T_2^2 >= t^4\,[1-4\frac{1+z}{z^3}(-z+\frac{z^2}{2}-\frac{z^3}{3}+\frac{z^4}{4}+\ln(1+z))] \quad , \qquad \text{(II-26d)}$$

where $z = v_y t$. The final result can be written as:

$$(\delta g')^2 = \frac{180(1+v_y t)\,\sigma_z^2}{Nt^4}h(v_y t) \quad \text{or} \quad (\delta y_0)^2 = \frac{y_0^4}{t^4}\frac{180(1+v_y t)\sigma_z^2}{(g/2)^2 N}h(v_y t) \quad , \quad \text{(II-27)}$$

where $h(z)$ is a rational combination of the functions given in Eq. (II-26a)-(II-26d).

There are three points to mention in regards to Eq. (II-27). First, the ratio y_0/t in the equation is no longer a constant even for a full field of view trajectory. In fact, for a 60-degree field-of-view sensor, the time in the field of view is always reduced for an approaching shot (and increased for a receding shot) compared to the crossing shot at the same velocity and initial range, y_0. The geometry of the shot determines the time in the field of view, and this is the most important variable in Eq. (II-27).

Second, the factor $1 + v_y t = y_e/y_0$ is the ratio of the y-coordinate when the projectile leaves the field of view, y_e, and its initial coordinate. For approaching shots, this factor is less than one and reduces the variance. This is easily understood since as the object approaches the focal plane, the angular displacements are magnified. This is the second most important factor since for approaching shots, it can reduce the variance substantially.[6]

---

[6] Note, however, that in the limit of $v_y t = -1$, for which this factor equals zero, the approximation that the value of v_y is precisely known breaks down and the variance given in Eq. (II-27) is only a lower bound to the true variance. A separate calculation may be performed for that limit but the error given here remains a rigorous lower bound.

Third, the detailed behavior of the moment functions in Eq. (II-26). The function h(z) used in Eq. (II-27) is plotted in Fig. II-1a. It is remarkably constant for z > – 0.5. For small z (= $v_y t$), it can be written as:

$$h(z) = 1 + 13 z^2 / 105 \quad .$$

(II-28)

The value of h(z) and the quadratic approximation are shown in Fig. II-1b. As z => – 1 (for which the bullet trajectory nearly intercepts the sensor), h(z) increases rapidly proportional to 1/(1+z); the product (1+z)h(z) has a limiting value of 1/15.

The reduced value of the error for direct shots (z => – 1) must be taken with a grain of salt since the extrapolation error for such shots (for which the initial flash may be unobserved) is in the same direction and is certainly larger. Thus, there is a possible additional error of up to 100 meters to be added to the direct shots. If one wanted to combine the extrapolation error with the range error one might write

$$(\delta y_0)^2 = \frac{y_0^4}{t^4} \frac{180(1 + v_y t)\sigma_z^2}{(g/2)^2 N} h(v_y t) + (\delta E)^2 \sin^2 \beta \quad ,$$

(II-29)

where β is the angle between the trajectory and the x-axis ($\beta = 0$ for crossing shots). For direct shots, $\pi/2 \geq \beta \geq (\pi - \Omega)/2$ (90 > β > 60 degrees for the notional sensor) and the extrapolation error will dominate. Of course, if the complete trajectory is visible, then the extrapolation error is relatively small, being determined only by the sample rate.
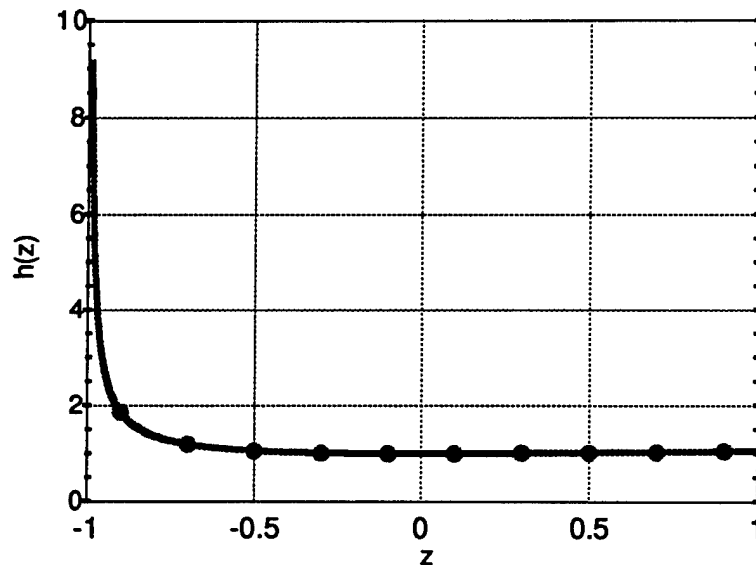

Figure II-1a.   Correction Function h(z), z = $v_y t$
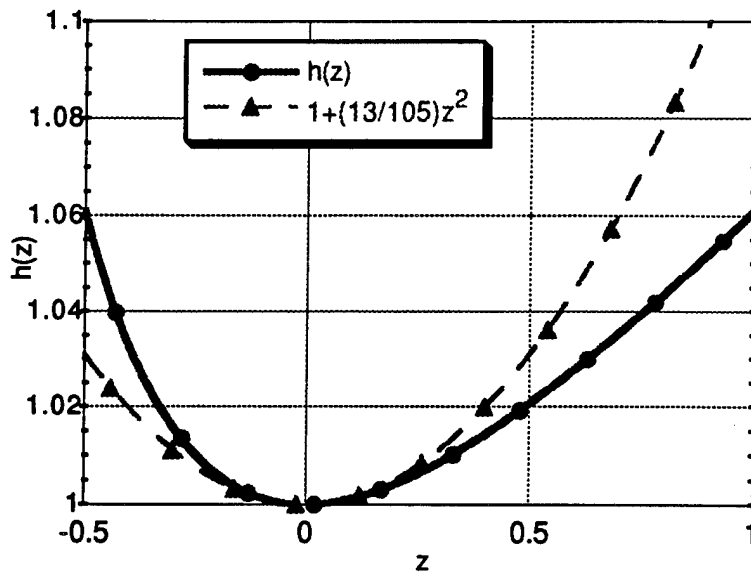
Figure II-1b.   Correction Function h(z) and Quadratic Approximation

The numerical factor 180 (1+z)h(z) is shown in Fig. II-2a.   It decreases nearly linearly with a final value of 12 at z = – 1 (but with a logarithmically singular derivative: at z = – 0.99 the value is greater than 16).   This provides a correction factor to the range error estimates given by the square root of (1+z)h(z) as shown in Fig. II-2b.   For the extreme shots the factor is about 0.4 for z = – 0.9 and has a limiting value of 0.26 at z = – 1.

Figure II-2a.   Numerical Factor in Range Variance as a function of z = $v_y t$

II-11

Figure II-2b. Range Error Correction Factor as a function of $z = v_y t$

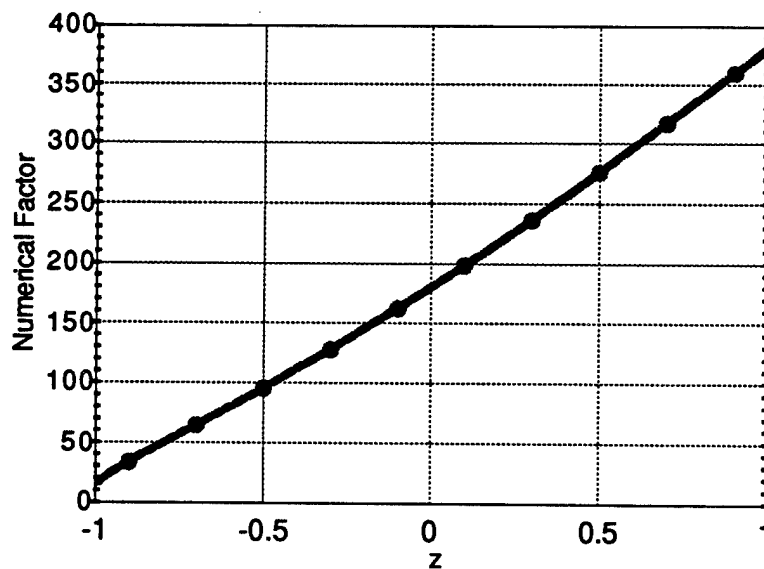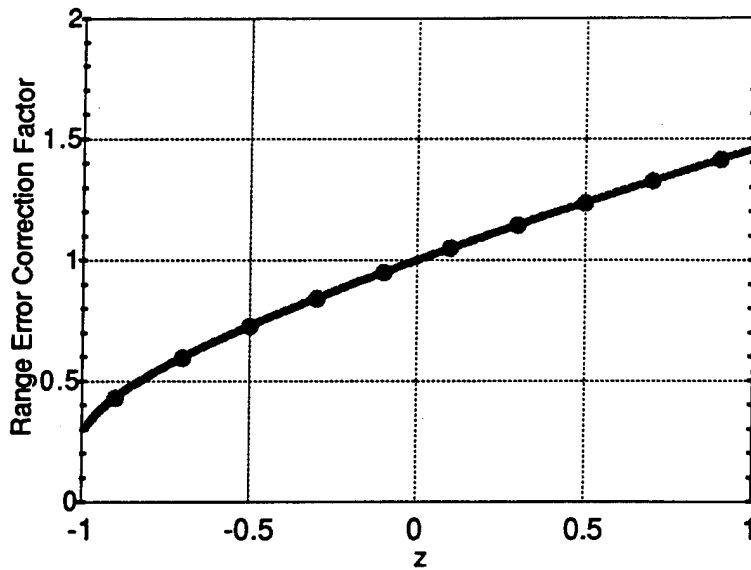The precise value of the range error depends on the geometry of the shot. Consider the paths shown in Fig. II-3 for the 60-degree sensor. For a shooter located at points A and B, the crossing shot is indicated by "a_1" and "b_1", respectively. These crossing shots have the values given for various ranges and initial velocities in Table II-1. For the shots with an angle of 30 degrees inward (denoted "a_2" and "b_2" in Fig. II-3), the values of y_e/y_0 are 1/2 and 3/4, respectively, and the error variance is proportionally reduced. However, the length of these paths is smaller than the a_1 and b_1 paths by a factor of $\sqrt{3}/2$, increasing the variance by a factor of $(\sqrt{3}/2)^5 = 2.1$. The correction factors are therefore approximately 1.05 and 1.25 when applied to the corresponding columns in Table II-1. For the shots directed at the sensor from position A (denoted "a_3"), the range reduction is a factor of 0.26 for a direct hit (somewhat larger for near misses). For a shot originating at any other position, the variance is increased by the 5/2 power of the ratio of time of flight. For example, for position B ("b_3"), the time in the field of view is reduced by a factor of $\sqrt{3}/2$ and the variance is increased by a factor of 2.1. The overall correction factor is 0.37.
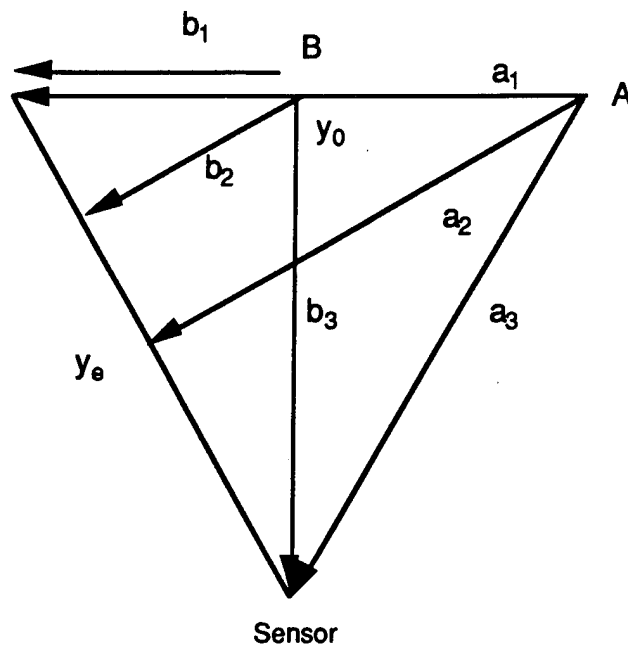
Figure II-3. Geometry of a Slant Shot

Table II-2 gives the correction factor to be applied to Table II-1 (using the second and third columns for the crossing and mid shots originating at A and B, respectively, and an example out of that table for each of these cases). For the direct shots, the correction factor is applied to the corresponding a1 case. Note that these errors do not include the extrapolation error which may dominate in the direct shot cases.

Table II-2. Geometric Corrections

Shot Geometry	Table II-1 Correction	$u_0 = 600$ m/sec, $y_0 = 250$ m
Crossing Shot-Full FOV: a_1	1	$\delta y_0 \approx \pm 27$ m
Crossing Shot-1/2 FOV: b_1	1	$\delta y_0 \approx \pm 150$ m
Mid Shot-Full FOV: a_2	1.05	$\delta y_0 \approx \pm 28$ m
Mid Shot-1/2 FOV: b_2	1.25	$\delta y_0 \approx \pm 188$m
Direct Shot: a_3	0.26	$\delta y_0 \approx \pm 7$ m
Direct Shot: b_3	0.37	$\delta y_0 \approx \pm 10$ m

III. INFLUENCE OF DRAG

A. LINEAR DRAG MODEL

A linear drag model is adopted. This is, in fact, a good approximation to the total force on the bullet in the supersonic regime (Mach number between 1.25 and 3, see Appendix A; the value of the drag force coefficent α for an M-16 rifle with standard ammunition was measured in one experiment to be approximately 0.56) and is mathematically simple. The further advantage of a linear model is that the vector components of the velocity are independent of one another. Writing the drag force as

$$\vec{F} = -\alpha \vec{u} \quad , \tag{III-1}$$

the motion of the projectile is given by:

$$x_i = x_0 + u_{x0}T_1 \tag{III-2a}$$

$$y_{ii} = y_0 + u_{y0}T_1 \tag{III-2b}$$

$$z_i = z_0 + u_{z0}T_1 - gT_2/2 \quad , \tag{III-2c}$$

where T_1, T_2, etc., are given by the truncated exponential functions

$$T_1 = (1 - e^{-\alpha t})/\alpha \tag{III-3a}$$

$$T_2 = 2!(e^{-\alpha t} - 1 + \alpha t)/\alpha^2 \tag{III-3b}$$

$$T_3 = 3!(1 - \alpha t + (\alpha t)^2/2! - e^{-\alpha t})/\alpha^3, \text{ etc.} \tag{III-3c}$$

The estimation problem now includes the value of the viscous drag coefficient α. The azimuthal and elevation degrees of freedom are coupled together by the α estimate even for the crossing shot. However, for nearly horizontal shots, it is clear that it is primarily the horizontal motion that permits the drag coefficient to be estimated. Section III-B shows that the drag coefficient can be adequately estimated from the horizontal motion alone and can be assumed to be known for the vertical coordinates. Section III-C applies the resulting drag model to the crossing-shot case. Finally, Section III-D combines the drag effects with the non-crossing shot geometry.

B. ESTIMATE OF THE DRAG COEFFICIENT

It can be shown that the horizontal motion gives a very accurate estimate of α. To see this most simply, consider the pixel motion, expanded for small values of the time t:

$$X_i \sim x' + v_{x0} t_i - v_{x0} \alpha t_i^2 / 2 \qquad \text{(III-4a)}$$

$$Z_i \sim z' + v_{z0} t_i - v_{z0} \alpha t_i^2 / 2 \quad . \qquad \text{(III-4b)}$$

The expression for the horizontal motion (III-4a) is formally just like the zero drag vertical estimation problem or the y-velocity estimation of the previous section. Thus, one has immediately:

$$(\delta v_{x0}\alpha)^2 \approx 180 \, \sigma^2 / (N \, t^4) \quad . \qquad \text{(III-5)}$$

For a field of view of approximately one radian, the angular velocity is $v_{x0} \sim 1/t$, so that

$$(\delta \alpha)^2 \approx 180 \, \sigma^2 / (N \, t^2) \quad . \qquad \text{(III-6)}$$

Thus, for transit times of the order of 1 sec, $N \sim 400$ and $\delta \alpha \sim \sigma \approx 0.25 \, 10^{-3}$; since the value of α is O(1), this is better than 1 part in 4,000.

This error is insufficient to induce a significant error in the estimation of range. If there is an error in α, then again using a perturbational approach to estimate effects, the error in g' is roughly

$$\delta g' \approx - v_{z0} \, \delta\alpha \quad . \qquad \text{(III-7)}$$

The total error includes the statistical error calculated as in the previous section and the error of Eq. (III-7); treating these as statistically independent,

$$(\delta g')^2 = [1 + (v_{z0} / v_{x0})^2] 180 \, \sigma^2 / (N \, t^4) \quad . \qquad \text{(III-8)}$$

For nearly horizontal shots, the contribution of the drag error is clearly negligible. Therefore it is sufficient to assume that the viscous drag coefficient is known. This has the advantage of reducing the problem to a three parameter linear estimate for the crossing shot and gives an accurate lower bound to the range error.

C. EFFECT OF DRAG ON THE ESTIMATE

Assuming that the drag coefficient is exactly known, the solution is immediate. The formal solution of the estimation is identical to the zero-drag case

$$(\delta g')^2 = \sigma^2 / [N(\sigma_2^2 (1 - \rho^2))] \quad . \qquad \text{(III-9)}$$

Calculating the statistical averages needed:

$$< T_1 > = T_2/2t \tag{III-10a}$$

$$< T_2 > = T_3/3t \tag{III-10b}$$

$$< T_1 T_2 > = T_2^2/4t \tag{III-10c}$$

$$< T_1^2 > = [T_2 - T_1^2]/2\alpha t \tag{III-10d}$$

$$< T_2^2 > = [2t\,T_3/3 - T_2^2/2 - T_4/6]/\alpha t \quad . \tag{III-10e}$$

Using these expression to define the values of ρ and σ_2, one obtains

$$(\delta g')^2 = [\ 180\ \sigma^2/\,Rt^5\ ]\ f(\alpha t) \quad , \tag{III-11}$$

where $f(\alpha t)$ is a rational function of the expressions in Eqs. (III-10a)-(III-10e) For small value of αt:

$$f(\alpha t) = 1 + (\alpha t)^2/42 \quad . \tag{III-12}$$

Figure III-1 shows that this form is a good approximation for $\alpha t < 5$.
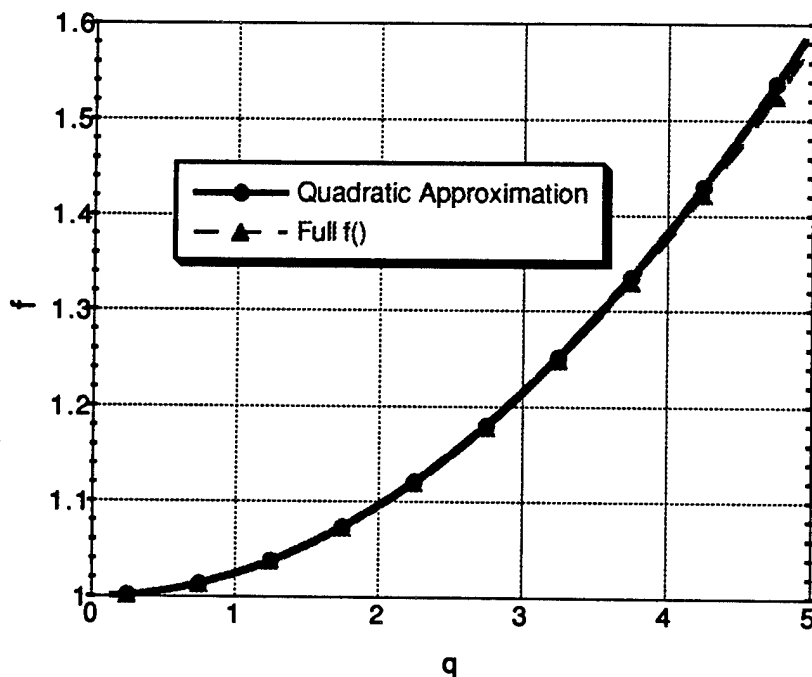

Figure III-1. "f" Drag Factor as a Function of q = αt

The effect of the drag on the form of the variance is therefore almost negligible. The primary effect is the slowing down of the velocity and the concomitant increase in the time spent in the field of view. The average velocity, $\overline{u}_0$, is given by:

III-3

$$\overline{u}_0\,(\alpha t) = u_0\,(1 - e^{-\alpha t})/\alpha t \quad . \tag{III-13}$$

The final result for the variance in the estimate of range is therefore:

$$(\delta y_0)^2 = \{720\,\sigma^2\,\overline{u}_0{}^5 \,/\,[g^2\,R\,y_0\,(2\,\tan\,(\Omega/2))^5]\,\}f(\alpha t) \quad . \tag{III-14}$$

The results given in Table II-1 can be used without change (neglecting the f() correction) if the velocities are interpreted as the average velocity over the field of view. For any particular trajectory, the time of transit and expected value of the drag coefficient should be used to provide an estimate of the average velocity. It is expected that αt will be of order 1, probably less than 0.5 for shorter ranges.

For $\alpha t = 1$, the average velocity is 63 percent of the initial velocity (the final velocity is 37 percent of the initial velocity). For a high velocity bullet (initial velocity 1,000 m/sec) the average is reduced to approximately 600 meters/sec; for a low velocity (initial velocity 700 m/sec), it is reduced to approximately 440 m/sec.

For $\alpha t = 0.5$, the average velocity is 79 percent of the initial velocity (the final velocity is 60 percent of the initial velocity). For a high velocity bullet (initial velocity 1,000 m/sec), the average is reduced to 790 meters/sec; for a low velocity (initial velocity 700 m/sec), it is reduced to approximately 555 m/sec.[7]

For the M-16 case described in Appendix A, $\alpha = 0.56$, so αt is approximately 0.44 after 500 meters of flight. The average velocity over the first 500 meters for the M-16 case is 650 meters/sec.

D. COMBINING DRAG WITH SLANT SHOTS

With the machinery in place for non-crossing shots with no drag and crossing shots with drag it is straightforward to write down the general result. It will be assumed that the projective y-velocity and drag coefficient are estimated from the horizontal motion as above. The errors in the y-velocity and drag coefficient will be larger than in the two previously discussed limiting cases, but a preliminary analysis indicates that the increase in error is not large; one is simply increasing the number of parameters to be estimated from

---

[7]   Note that if the velocity of the bullet approaches Mach 1, the linear drag model and indeed any simple drag model will become inappropriate (near Mach 1, the effects of drag on the bullet are likely to be difficult to model). Estimates of α are in the vicinity of 1.25 (see Appendix A) for typical projectiles. At 250 meter range and for the full field of view crossing shot geometry, a 700 m/sec projectile will transit in approximately 0.3 seconds, so that $\alpha t \approx 0.45$. In this case, the final velocity will be 420 m/sec, which is still in the linear regime.

the horizontal motion. However, assuming that these quantities are known does ignore some of the error sources in the full problem. Therefore, the estimates of the error given below are a lower bound to the range estimates, but it is one we believe is reasonably accurate except for direct or near direct shots for which the horizontal motion is reduced.

Averages are defined by

$$< F(t) >= \frac{\int_0^t \frac{dt\, F(t)}{(1+v_y T_1)^2}}{\int_0^t \frac{dt}{(1+v_y T_1)^2}} = \frac{\int_0^t \frac{dt\, F(t)}{(1+v_y T_1)^2}}{\|w\|} \quad , \qquad \text{(III-15a)}$$

where the normalizing weight $\|w\|$ is

$$\|w\| = \int_0^t \frac{dt}{(1+v_y T_1)^2} = \frac{v_y}{v_y + \alpha}[\frac{T_1}{1+v_y T_1} + \frac{\alpha/v_y}{v_y + \alpha}[\ln(1+v_y T_1) + \alpha t]] \quad . \qquad \text{(III-15b)}$$

The error in range is given by

$$(\delta y_0)^2 = \frac{t\, y_0^4\, \sigma_z^2}{N\, \|w\|\, (g/2)^2 \sigma_2^2\, (1-\rho^2)} \qquad \text{(III-16a)}$$

$$(\delta y_0)^2 = \frac{180\, t\, y_0^4\, \sigma_z^2}{N\, \|w\|\, (g/2)^2 t^4}\, p(\alpha t, v_y t) \quad , \qquad \text{(III-16b)}$$

where the averages, standard deviations and correlation parameters are calculated with the average defined as in Eq. (III-15); note that $\|w\|$ is proportional to t for t small. The function $p(\alpha t, v_y t)$ in Eq. (III-16b) is a rational function of the various moments computed with the weight factor. This form reduces to the previous results in each special case; for zero drag $p(0, v_y t) = h(v_y t)$ and for crossing shots $p(\alpha t, 0) = f(\alpha t)$. The integrals now required to evaluate $p(\alpha t, v_y t)$ cannot be evaluated in terms of a finite number of elementary functions, but special cases can be evaluated by expanding the integrals.

For small values of time (meaning αt and/or $v_y t$ are small), the weight factor $t / \|w\|$ may be written as

$$\frac{t}{\|w\|} = (1+v_y T_1)(1+\frac{\alpha v_y}{6} T_1^2) \quad . \qquad \text{(III-17a)}$$

The second factor could use either t or T_1 interchangeably; the first factor is just the value of y_e/y_0 in the presence of drag. The statistical factors again only weakly depend on the parameters,

$$p(\alpha t, v_y t) = (1 + \frac{13}{105}(v_y t)^2 + \frac{(\alpha t)^2}{42}) + O(t^3) \quad , \tag{III-17b}$$

so that the error can be written as

$$(\delta y_0)^2 = \frac{y_e}{y_0} \frac{180 \; y_0^4 \; \sigma_z^2}{N \; (g/2)^2 t^4}(1 + \frac{13}{105}(v_y t)^2 + \frac{(\alpha t)^2}{42} + \frac{\alpha v_y t^2}{6}) \quad . \tag{III-17b}$$

The correction terms in the last factor are all small for $v_y t > -0.5$. Therefore in this region, the results of the previous sections can be applied using the average velocity. Thus, the correction factors due to geometry of Table II-1 are appropriate for the crossing and mid shots (and the numerical example is correct if the *average* velocity is 600 meter/sec).

For the nearly direct shots for which $v_y t \Rightarrow -1$, a different expansion of the integrals is required. The details of this calculation are uniformative but the final result can be written as:

$$(\delta y_0)^2 = \frac{12 \; (|u_{y0}|e^{-\alpha t})^5 \; \sigma_z^2}{R \; y_0(g/2)^2} I_d(\alpha y_0 / u_{y0}) \quad , \tag{III-18a}$$

where the function $I_d(\alpha y_0/u_{y0})$ is given in Appendix C and $I_d(0) = 1$. Note that factor $u_{y0} e^{-\alpha t}$ is the *final* velocity in the y-direction of the projectile.[8] To second order in the drag terms, Eq. (III-18a) can be written as:

$$(\delta y_0)^2 = \frac{12 \; (|u_{y0}|e^{-\alpha t})^5 \; \sigma_z^2}{R \; y_0(g/2)^2}(1 - \frac{11}{6}\alpha y_0 / u_{y0} + \frac{371}{135}(\alpha y_0 / u_{y0})^2 + ...) \quad . \tag{III-18b}$$

In terms of the *average* velocity of the projectile in the y-direction, this can also be written to first order in the drag as:

$$(\delta y_0)^2 = \frac{12 \; | \bar{u}_{y0}^5 | \; \sigma_z^2}{R \; y_0(g/2)^2}(1 + \frac{2}{3}\alpha y_0 / u_{y0}) \quad . \tag{III-18c}$$

The perturbational result converges slowly. As a simple mnemonic, one sees by comparing Eq. (III-18b) and Eq. (III-18c) that the effect of drag is to lower the effective velocity from the non-drag case; the result is bracketed by neglecting the perturbational terms and using two different velocities: the final velocity gives an underestimate of the range variance and the average velocity an overestimate (recall that $u_{y0} < 0$ for this case). The precise value can be computed numerically from the integrals given in Appendix C.

---

[8]   One may also write ex($-\alpha t$) as $1 + \alpha y_0/u_{y0}$ (this is exact for direct shot trajectories).

IV. CONCLUSIONS

The rigorous error estimates given here do not preclude the use of a system similar to the proposed system for estimating the parameters of a high-speed bullet trajectory. Indeed, in the absence of a more complete sensor design and a more detailed system description describing the action to be taken in response to the shooter, it is difficult to quantify completely the abilities and limitations of the concept. However, the errors calculated indicate that the system needs higher resolution than that suggested to provide sufficient range accuracy to be militarily useful. The differences between these analytical calculations and informally reported simulation results may possibly be attributed to the effects of the strong correlation between the estimates of the vertical velocity and gravitational contributions.

The calculations have shown that the system is capable of producing highly accurate information about the track in angular or projective coordinates: only the range itself is in doubt. Thus, any method of deducing range in addition to the direct estimate provided by the track might permit a more accurate location. For example, battlefield intelligence and terrain considerations combined with knowledge of the weapons being used on the battlefield (and hence the possible values of the absolute muzzle velocities), might provide sufficient additional information to provide a useful estimate of range.

The estimates made are maximum likelihood estimates, and hence provide rigorous bounds on the errors. For the zero-drag crossing shots, the errors given were made with no approximations other than assuming that the pixel location errors were normally distributed. For drag and non-crossing shot cases, it was assumed that the drag coefficients and the projective y-component of the velocity were exactly known (since they can be estimated accurately from the horizontal motion of the projectile). This means that the error estimates are lower bounds to the true error; that is, the true error can only be larger than that given here.

The results are summarized here for convenience. The answer for the most general case of non-crossing shots with drag involve some tedious integrals. For shots that do not deviate too much from crossing shots (ending y-coordinate, y_e, no less than 1/2 the initial y-coordinate, y_0), the result is well approximated by:

$$(\delta y_0)^2 = \frac{y_e}{y_0} \frac{180}{N} \frac{y_0^4 \, \sigma_z^2}{(g/2)^2 t^4} (1 + \frac{13}{105}(v_y t)^2 + \frac{(\alpha t)^2}{42} + \frac{\alpha v_y t^2}{6}) \quad , \qquad \text{(IV-1)}$$

where $v_y = u_{y0}/y_0$ is the projective y-component of the velocity. For direct shots a first approximation to the integrals gives:

$$(\delta y_0)^2 = \frac{12}{R} \frac{(|u_{y0}|e^{-\alpha t})^5 \, \sigma_z^2}{y_0(g/2)^2} (1 - \frac{11}{6}\alpha y_0 / u_{y0} + \frac{371}{135}(\alpha y_0 / u_{y0})^2 + ...) \quad . \quad \text{(IV-2)}$$

The range error depends on the sensor parameters chosen and the geometry of the shot. Figure IV-1 repeats Fig. II-3 to illustrate some common shot geometries.
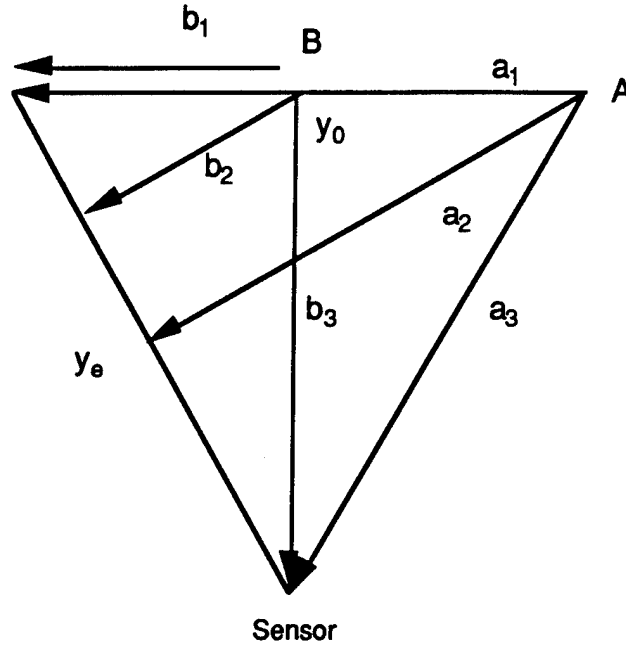
Figure IV-1. Shot Geometry

Table IV-1 gives the range errors expected for the assumed sensor parameters and a typical range of 250 meters and *average* velocity of 600 meters/sec. The results scale as the 5/2 power of the velocity and inversely as the square root of the range. Thus, for slower projectiles at longer ranges the error will be reduced. The direct shot errors do not include the drag correction in Eq. (IV-2) because the perturbation expansion clearly has not converged; note also that the error for direct shots is likely only to be a lower bound.

Table IV-1. Range Errors

Shot Geometry	$u_0 = 600$ m/sec, $y_0 = 250$ m
Crossing Shot-Full FOV: a_1	$\delta y_0 \approx \pm 27$ m
Crossing Shot-1/2 FOV: b_1	$\delta y_0 \approx \pm 150$m
Mid Shot-Full FOV: a_2	$\delta y_0 \approx \pm 28$m
Mid Shot-1/2 FOV: b_2	$\delta y_0 \approx \pm 188$ m
Direct Shot: a_3	$\delta y_0 \approx \pm 7$ m
Direct Shot: b_3	$\delta y_0 \approx \pm 10$ m

This table shows that a reduction in the field of view is an important factor in the overall error. In urban or other cluttered environments the field of view may be sharply restricted. For example, in a city the effective field of view decreases with range. For a sniper in an urban location the observable path of the bullet may be restricted to 120 meters (a distance across a park) to 30 meters (a distance across a street). For an average velocity of 600 meters/sec, this corresponds to a time ranging from 0.05 to 0.2 seconds. Using 0.1 second as a typical value (60 meters at 600 meters/sec) and the sensor parameters given above, the error in a near crossing shot is:

$$\delta y_0 = 2.2 \ 10^{-2} \ y_0^2 \ . \qquad \qquad \text{(IV-3)}$$

At a range of 100 meters, the error is $\delta y_0 = \pm 220$ meters and increases with range. At 200 meters the error is $\delta y_0 = \pm 880$ meters. These errors are sufficiently large to severely limit the usefulness of the concept in urban scenarios, even with a marked improvement in resolution.

These errors are lower bounds. The largest error omitted is the extrapolation error if the initial flash is unobserved. This may be as much as 100 meters and is the dominant source of error in the range for direct shots. Other sources of error have also been omitted such as possible bullet tumbling and lift that would complicate the calculation of the error. It was also assumed that the orientation of the sensor is known precisely. This leads to a systematic error in the orientation of the track but does not change the statistical variance around the presumed track. For example, if the sensor orientation is in error by 1 milliradian, this corresponds to a 1 milliradian rotation of the estimated track.

An alternate way of viewing the results is to relate the range error to the angular track error. Using the depression angle as an example:

$$(\delta g')^2 = \frac{(\delta v_z)^2}{v_x^2} \frac{v_x^2 \sigma_1^2}{\sigma_2^2} \quad . \tag{IV-3a}$$

Using the zero-drag and near crossing shot limit for convenience (the result is essentially unchanged in the presence of drag),

$$5\delta y_0 = \delta\Theta_z \frac{v_x y_0^2}{t} = \delta\Theta_z \frac{u_{x0}^2}{\Omega} \quad , \tag{IV-3b}$$

where $\Theta_z = v_z/v_x$ and $\Omega = v_x t$ is the projective distance (angle) traveled. Therefore, for a nominal 1000 km/sec, the needed track resolution would be

$$\delta\Theta_z = 5\Omega\delta y_0 \text{ microradians} \quad . \tag{IV-3c}$$

Thus for 1 meter accuracy in the range and a 1/2 radian trajectory, a 2.5 microradian overall track error would be required; for 10 meters, 25 microradians.

APPENDIX A

DRAG FORCES ON BULLET PROJECTILES

APPENDIX A
DRAG FORCES ON BULLET PROJECTILES

Although often described as a quadratic force, the dependence of the coefficient of the quadratic term on the velocity leads to a linear drag force in the region of observation. Figure A-1 illustrates this point with a plot of drag force versus Mach Number, computed from the data on drag coefficients for projectiles presented in Fig. 30, Chapter XVI, of Hoerner's book on Fluid-Dynamic Drag.* The details of the curvature depend upon the relative sizes of the wave drag and base drag, since the skin drag is usually small in this region. Therefore, extrapolating the drag along the flight path outside the field of view will require knowledge of the bullet type. In principle, detailed and accurate enough measurements might support creating a realistic extrapolatable model for the drag.
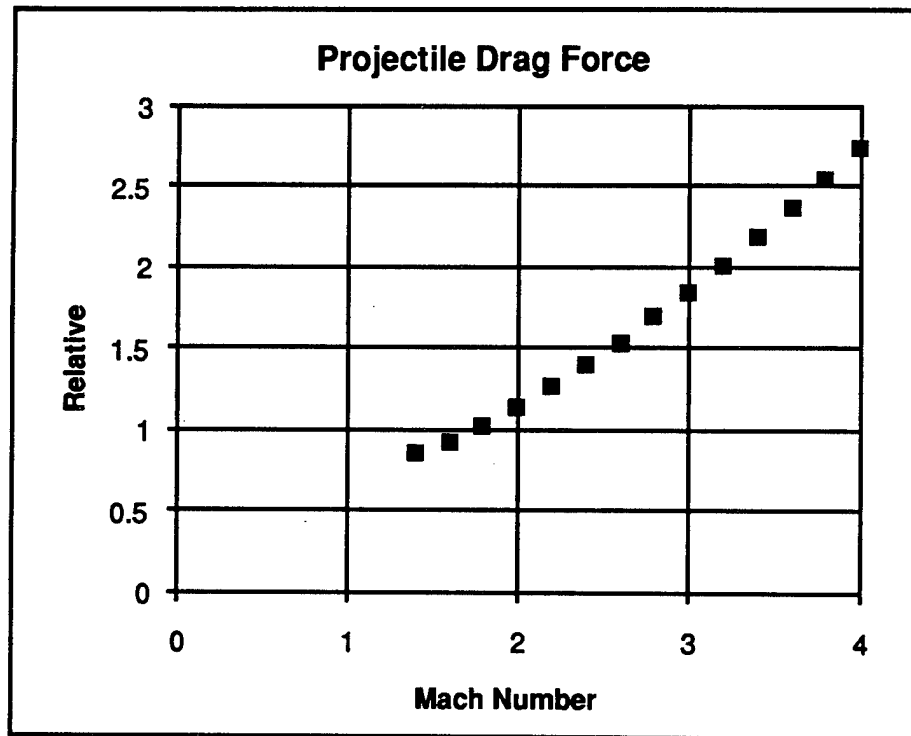

Figure A-1. Drag Force as a Function of Velocity

---

* Sighard F. Hoerner, Dr.-Ing., *Fluid Dynamic Drag: Practical Information on Aerodynamic and Hydro-dynamic Resistance* (Midland Park, N.J.: self published), 16–21.

Figure A-2 shows data provided by the Ballistics Research Laboratory for an M-16. The initial velocity was approximately 804 m/sec dropping to 520 m/sec after about 0.8 second. An exponential model with $\alpha = 0.56$ provides an excellent fit to the data.
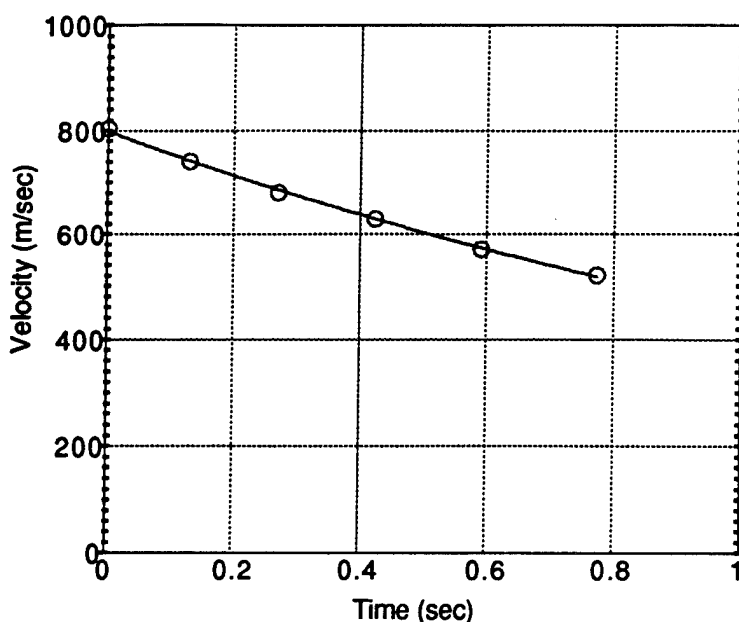

Figure A-2. Velocity of M-16 Ball Ammunition

Another major issue beyond the statistical treatment in the body of this draft is whether or not a three-dimensional track could be accurately extrapolated out of the field of view to a firing position in the case where the firing position were unknown. Clearly this requires knowledge of the muzzle velocity. While muzzle velocities for a given gun and ammunition have low variances, the large number of available weapons and ammunition types makes a priori knowledge of the muzzle velocity unlikely. For example, *Jane's Infantry Weapons* lists about 40 rifles which fire standard NATO 7.62 × 51 mm ammunition. As shown in Table A-1, the muzzle velocities range from 700 m/s to 860 m/s. This corresponds to a 20 percent uncertainty in the distance at which the bullet was first seen, if one is attempting to use prior knowledge of the velocity to distinguish the track. Furthermore, when extrapolating outside the field of view, the difference in firing position if one extrapolates back to 700 m/s versus 860 m/s will be on the order of 100 m. Machine guns firing this size ammunition have a smaller range of muzzle velocities, from 790 m/s to 869 m/s. On the other hand, if one does not know cartridge length, but only caliber, then machine gun muzzle velocities also extend down to 700 m/s and rifle muzzle velocities extend down to 572 m/s.

A-4

Table A-1. Rifle Velocities

Rifles		
Country	Title	Muzzle Velocity (m/s)
5.56 × 45 mm		
Iraq	Tabuk	710 (minimum)
USA	Ruger AC-556	1058 (maximum)
7.62 × 39 mm Soviet		
Hungary	AMD-65	700 (minimum)
Finland	Valmet M90	800 (maximum)
7.62 × 51 mm NATO		
Japan	Type 64	700 (minimum)
Austria	Steyr SSG-69	860 (maximum)
Austria	Steyr Police	860 (maximum)

Machine Guns		
Country	Title	Muzzle Velocity (m/s)
5.56 × 45 mm		
Israel	Galil ARM	850 (minimum)
Austria	Steyr LSW	1000 (maximum)
Canada	C7	1000 (maximum)
Yugoslavia	M82	1000 (maximum)
7.62 × 51 mm		
Switzerland	SIG 710-3	790 (minimum)
USA	M134	869 (maximum)
12.7 × 99 mm (.50)		
USA	Browning M2HB	810 (minimum)
Belgium	FN M2HB	930 (maximum)
Belgium	FN M2HB/QCB	930 (maximum)

APPENDIX B

SENSOR CONSIDERATIONS

APPENDIX B
SENSOR CONSIDERATIONS

In the absence of a completely specified sensor design concept, an analysis would be supererogatory. The points mentioned here form a prolegomenon to a thorough analysis.

A 512×512 MWIR focal plane is likely to be at most 2 cm in size. For a 60 degree field of view, this corresponds to a focal length of 2 cm and a maximum practical (f#1) aperture of 2 cm. For a wavelength of 4 microns, the size of the blur circle matches the detector subtense for an aperture of 1/2 cm (f#4). For a sensor with an aperture greater than 1/2 cm, the blur spot will be proportionally smaller than the detector and highly precise subpixel location accuracy is unlikely unless the blur spot is deliberately defocused.

Assuming the blur circle is small compared to the pixel height (f# < 4, no defocusing), the only possible assignment of the z coordinate is the center of that pixel (vertically). Assuming the center of the image could be anywhere within the pixel, the vertical error is $1/\sqrt{12}$ pixel ≈ 0.29 pixel. However, the localization errors between samples are not independent as assumed in the text. Therefore, one would not get the benefit of the factor of N (100–400) but rather a much smaller gain of the order of 2 or 3 (since the number of rows crossed by the projectile will be 2 or 3 at most. Therefore, the f# will have to be greater than f#4 and information between rows used to isolate the location.

In general, subpixel localization can depend on turbulent scintillation, distortion and blurring of the image of the projectile; hydrodynamic force perturbations on the trajectory (lift and cross-winds); and on the degree of non-uniformity of the focal plane. For example, for a path length of 1 km, and a 0.25 cm diameter optic (f#8, two samples/blur in the vertical), and moderate turbulence ($C_n^2 = 10^{-12}$), the short time exposure uncertainty in the centroid of the image is about 0.1 milliradian (1/20 pixel). The error due to turbulence increases proportionally to the square root of the range so that the ratio σ_{turb}^2/y_0, which is required in the development in the body of the paper, would be fixed. Thus, if the only limit to the subpixel localization were turbulence, the range error would become independent of range and might approach 1/5 of the errors given for $y_0= 1$ km in Table II-1; for

example, ± 30 meters for u = 800 meters/sec and a 30 degree field of view. This lower bound on the subpixel error might be increased by a factor of 3 in the most severe turbulence and does not take into account any distortion of the point spread function that might affect the estimate of the location, array non-uniformities, or any other source of error.

The readout rate corresponds to 100 megasamples/sec which is aggressive but has been used in special purpose focal planes such as the NWSC (Dahlgren Division) Non-uniformity correction (NUC) focal plane; the current cost of the NUC focal plane (as a limited production item) is in excess of $100,000. The cost would be expected to be reduced under production conditions. If the readout rate were reduced to 100 Hz, the range errors would double.

APPENDIX C

THE FACTOR I_d

APPENDIX C
THE FACTOR I_d

The formula given in Eq. (III-18a) for the direct shot in the presence of drag is

$$(\delta y_0)^2 = \frac{12}{R} \frac{(u_{y0}e^{-\alpha t})^5 \sigma_z^2}{y_0(g/2)^2} I_d(\alpha y_0 / u_{y0}) \qquad . \tag{C-1}$$

The function $I_d(x)$ is given by:

$$1/I_d(x) = \frac{-48}{\epsilon^2}[\frac{\epsilon^2}{3}\bar{t}^3(\epsilon) - i_2(\epsilon) + \bar{t}(\epsilon)(\bar{t}(\epsilon)+1) - \frac{(\frac{\epsilon\bar{t}^2(\epsilon)}{2} + \bar{t}(\epsilon) + i_1(\epsilon))^2}{\bar{t}(\epsilon)}] \quad , \tag{C-2}$$

where

$$\epsilon = \frac{x}{1+x} \tag{C-3a}$$

$$\bar{t}(\epsilon) = \frac{\ln(1-\epsilon)}{\epsilon} \tag{C-3b}$$

$$i_1(\epsilon) = \int_0^1 \frac{\ln(1-\epsilon r)}{-\epsilon r}dr \tag{C-3c}$$

$$i_2(\epsilon) = \int_0^1 \frac{\ln^2(1-\epsilon r)}{\epsilon r^2}dr \quad . \tag{C-3d}$$

These integrals result from taking the direct shot limit of the fundamental equations and some tedious algebra. Expanding the integral in Eq. (C-3a)–(C-3d) to second order and inserting the results into Eq. (C-2) gives the result given in the main text in Eq. (IIII-18b).

REPORT DOCUMENTATION PAGE

Public Reporting burden for this collection of information is estimated to average 1 hour per response, including the time for reviewing instructions, searching existing data sources, gathering and maintaining the data needed, and completing and reviewing the collection of information. Send comments regarding this burden estimate or any other aspect of this collection of information, including suggestions for reducing this burden, to Washington Headquarters Services, Directorate for Information Operations and Reports, 1215 Jefferson Davis Highway, Suite 1204, Arlington, VA 22202-4302, and to the Office of Management and Budget, Paperwork Reduction Project (0704-0188), Washington, DC 20503.

1. AGENCY USE ONLY *(Leave blank)*	2. REPORT DATE August 1995	3. REPORT TYPE AND DATES COVERED Final—January 1995–June1995

4. TITLE AND SUBTITLE

Error Analysis for Bullet Tracker Concept

5. FUNDING NUMBERS

DASW01 94 C 0054
T-Q2-893

6. AUTHOR(S)

Jeffrey Nicoll, David Sparrow

7. PERFORMING ORGANIZATION NAME(S) AND ADDRESS(ES)

Institute for Defense Analyses
1801 N. Beauregard St.
Alexandria, VA 22311-1772

8. PERFORMING ORGANIZATION REPORT NUMBER

IDA Paper P-3084

9. SPONSORING/MONITORING AGENCY NAME(S) AND ADDRESS(ES)

OSD (PA&E)
Land Forces Division
Pentagon, Room 2B256
Washington, DC 20301

10. SPONSORING/MONITORING AGENCY REPORT NUMBER

11. SUPPLEMENTARY NOTES

12a. DISTRIBUTION/AVAILABILITY STATEMENT

Approved for public release; distribution unlimited.

12b. DISTRIBUTION CODE

13. ABSTRACT *(Maximum 180 words)*

The ability to quickly locate a sniper's firing position from the bullet's track would be of use in both military and law enforcement applications. This paper addresses the question of how well a sniper could be located by observing the bullet's track with a modern high quality FLIR (forward looking infrared). If the muzzle flash is not observed the cross range uncertainty is driven by variations in possible muzzle velocity, and will be approximately 100 meters. The downrange uncertainty is driven by the need to distinguish a near, slow moving bullet from a far away faster moving bullet with the same angular velocity. This can be done in principle since the tracks have slightly different curvatures due to gravity. This requires observation of the track over a wide field of view in order to obtain an accurate determination of the curvature, and hence the range. Maximum likelihood estimates of the errors are presented for a variety of muzzle velocities, crossing angles, and fields of view. These results may be used in assessing different approaches to locating snipers.

14. SUBJECT TERMS

location of snipers, Operations Other Than War, projectile tracking

15. NUMBER OF PAGES

44

16. PRICE CODE

17. SECURITY CLASSIFICATION OF REPORT	18. SECURITY CLASSIFICATION OF THIS PAGE	19. SECURITY CLASSIFICATION OF ABSTRACT	20. LIMITATION OF ABSTRACT
UNCLASSIFIED	UNCLASSIFIED	UNCLASSIFIED	SAR